Use of a low energy accelerator to study mechanisms of track formation in plastic detectors: carbon ions in CR-39

J. Rickards, V. Romo, J.I. Golzarri, and G. Espinosa
Instituto de Física, Universidad Nacional Autónoma de México
Apartado postal 20-364, 01000 México, D.F., Mexico

Recibido el 18 de febrero de 2000; aceptado el 7 de abril de 2000

The Instituto de Física 3 MV 9SDH-2 Pelletron accelerator is being used to study the mechanisms of track formation and etching in plastic track detectors. With this type of accelerator controlled beams of many different ions can be produced. The technique used to obtain an adequate track density was to backscatter the ions from an Au film deposited on a thick vitreous carbon backing. In this way, at angles greater than 90° ions of masses $12 \leq m < 197$ amu will be backscattered in a clean monoenergetic beam. The energy is controlled by the accelerator energy (which allows the choice of several charge states, depending on the type of ion) and the scattering angle; the energy spectrum width is given by the thickness of the Au film. The ion fluence is controlled by the beam current, bombarding time and beam angle. Carbon ions with energies between 1 and 10 MeV were selected to impinge on CR-39 (allyl diglycol polycarbonate) plastic detectors, which were then chemically etched for different times and the track diameter recorded in 2 hour steps. Plots of diameter *vs.* ion energy and diameter *vs.* surface removal were obtained, and analyzed using track etch theory.

Keywords: Accelerator; carbon ions; CR-39; track production

El acelerador Pelletron de 3 MV (9SDH-2) del Instituto de Física ha sido usado para estudiar mecanismos de formación y grabado de trazas en detectores plásticos. Con este tipo de aceleradores se tienen haces controlados de diferentes iones. La técnica usada para obtener la densidad adecuada de trazas fue la de retrodispersión de iones de una película de oro depositada en un blanco vítreo de carbón. De esta forma, a ángulos mayores de 90°, para iones de masas entre 12 y 197 uam serán retrodispersados en un haz monoenergético. La energía es controlada por la energía del acelerador (la cual permite escoger de algunos estados de carga, dependiendo del tipo de ion) y el ángulo de dispersión; el ancho del espectro de energía está dado por el espesor de la película de oro. La afluencia de iones es controlada por la corriente del haz, tiempo de bombardeo y del ángulo del haz. Fueron seleccionados iones de carbono con energías entre 1 y 10 MeV, para ser implantados en CR39 (ADP), los cuales fueron grabados químicamente a diferentes tiempos, y los diámetros de las trazas leídos cada dos horas. Se obtienen y analizan las gráficas del diámetro de la traza contra energía del ion y las gráficas de diámetro de las trazas contra el desgaste superficial usando la teoría de trazas nucleares.

Descriptores: Acelerador; iones de carbono; CR-39; producción de trazas

PACS: 07.77.-n; 29.25.-t

1. Introduction

The detection of energetic ions by the formation of etched visible tracks in polymeric materials is finding increasing applications, due mainly to the simplicity and low cost of the method, and that it is well suited for measuring radiation doses. Many plastics have been tested [1], with widely varying results as to their usefulness. Their sensitivity to type of ion and ion energy are relevant parameters that can determine the range of applicability and under what conditions the detectors can be used as spectrometers.

The properties of the latent track formed when the ions penetrate the detector (projected range, ionization along the track, structural damage) can be calculated using computer codes like TRIM [2], that uses well known ion stopping theory in a Monte Carlo approach. On the other hand, theories on the etching mechanism that produces visible tracks from the latent tracks have also been developed [3–5]. However, more detail on how these mechanisms take place is desired, since until now most experiments have been done using ions from radioactive or fission sources, where the parameters may not be carefully controlled.

The Instituto de Física 3 MV Pelletron 9SDH-2 accelerator can produce monoenergetic ion beams of most elements. It is a two-stage machine into which negative ions are injected and positive ions are extracted, so the high voltage (variable up to 3 MV) is used twice for single-charged extracted positive ions and $(n + 1)$ times for positive ions of charge n. Therefore the energies available are in the 1 to 20 MeV interval, depending on the ions selected, and the ranges of the ions in a plastic detector will be approximately in the interval 1 to 20 μm. Energies (and ranges) can be varied continuously within these intervals. The purpose of this work is to assess the usefulness of this type of accelerator in investigating nuclear track detector material properties, and its application to the case of energetic carbon ions in CR-39 (allyl diglycol polycarbonate). Parallel experiments have been performed with nitrogen and oxygen beams [6, 7].

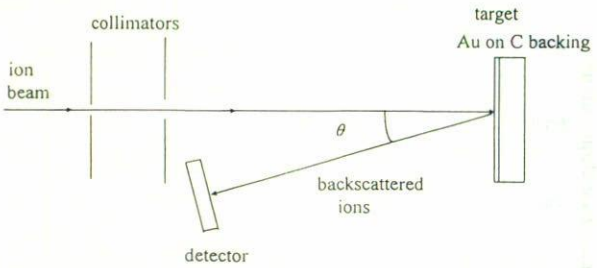

FIGURE 1. Carbon ions from the accelerator are backscattered from a thin Au film deposited on a thick C backing before impinging on the plastic detectors.

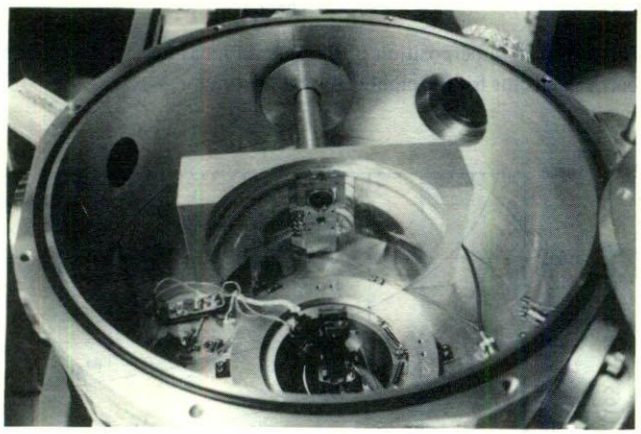

FIGURE 2. Spherical-shaped holder for experimental procedure.

2. Experiment

Since the beam intensity of the 3 MV Pelletron accelerator (nA to μA) is too high to be used directly on the detector materials, in this experiment the beam was elastically scattered from a target in a backward direction (Fig. 1) before impinging on the plastic detectors. The desired number of ions and their parameters are then varied by controlling the primary ion beam, and considering the scattering kinematics and cross sections. In the present case a carbon ion beam was obtained from the accelerator with energies varying between 1 and 12 MeV. The scattering geometry was selected with $\theta_{\rm lab} = 168°(\theta = 12°)$, and the detector was placed at a distance of 12.3 cm from the target, on a specially built spherical-shaped holder that ensures that the scattered ions arrive at the detector with normal incidence (see Fig. 2).

The target was a thin (85 nm) Au film deposited on a vitreous carbon backing. Its thickness was measured by He ion scattering. Under these conditions, for any primary beam of mass number A, a single monoenergetic group of ions will be scattered into the detector at $\theta_{\rm lab} = 168°$ o if their mass number is $12 \leq A < 197$. Ions with $A < 12$ will be scattered from the backing into the detector, providing an unwanted background; at the other extreme, masses with $A \geq 197$ will not be backscattered from either the Au film or the carbon backing.

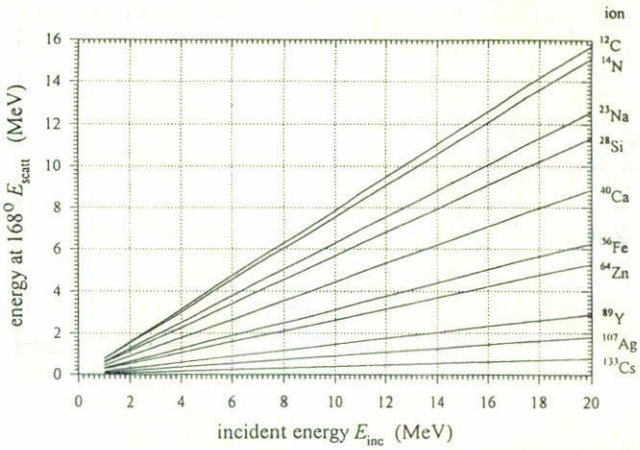

FIGURE 3. Energies of various ions elastically scattered from Au at 168°, as a function of incident (primary beam) energy, for the energies of the Pelletron accelerator.

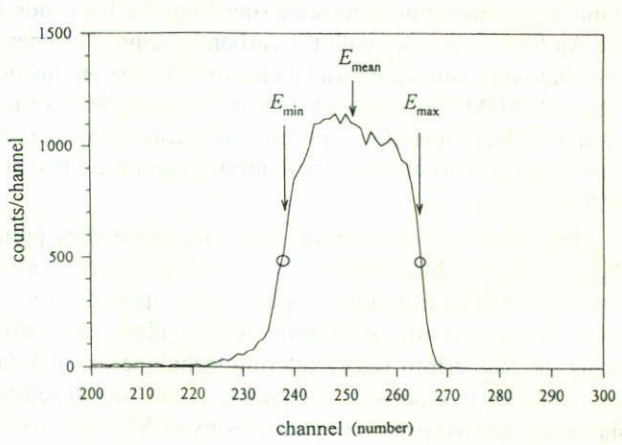

FIGURE 4. The shape of the peak measured with a surface barrier detector placed next to the plastic detector to monitor the experiment.

The energy of the ions that reach the detector is determined by scattering kinematics. Figure 3 shows the energies $E_{\rm scatt}$ of various easily available ions elastically scattered from Au at 168°, as a function of incident (primary beam) energy $E_{\rm inc}$, for the energies of the Pelletron accelerator. For each type of ion, if higher energies are desired, the scattering angle can be reduced. As a guide, if a scattering angle of 90° is selected, the kinematic factor $K = E_{\rm scatt}/E_{\rm inc}$ is 0.885 for ^{12}C ions and 0.194 for ^{133}Cs ions.

The ions that reach the detector will have an energy spread that depends on the thickness of the target. The shape of the peak in the energy spectrum is typically like that shown in Fig. 4, which was measured with a surface barrier detector placed permanently next to the plastic detector to monitor the experiment. The plateau is determined by the energy dependence of the Coulomb cross section. The position of the high energy point $E_{\rm max}$ (at 50% height) is given by the energy of ions scattered from the s urface of the Au film; the low energy

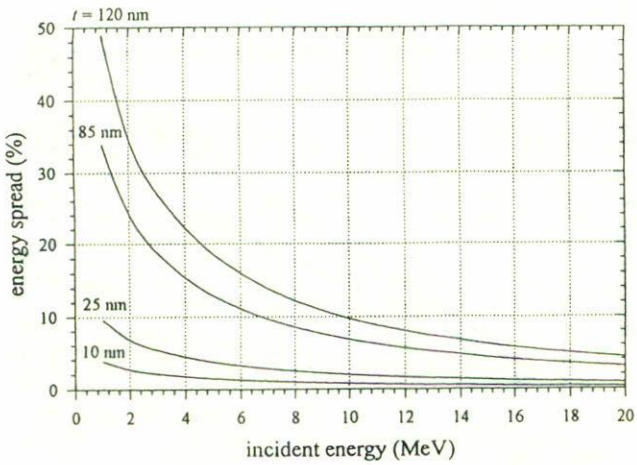

FIGURE 5. The energy spread, in energy, for C ions on Au films of different thicknesses.

point $E_{\min}$ corresponds to scattering from the back side of the Au film, in contact with the carbon backing. The energy distribution is convoluted with an assumed Gaussian function whose FWHM contains contributions from the detector resolution (which does not apply for the plastic detector), the beam energy resolution (after scattering) and the finite size of the detector.

The difference between the high and low energy points $E_{\max} - E_{\min}$, which is the main cause of the energy spread, can be calculated from ion stopping theory applied to the ion paths before and after scattering, as is regularly done when using the Rutherford Backscattering technique on thick targets [8]. For this purpose a computer code was developed that uses the electronic stopping powers of Montenegro [9], who provide a closed expression that can easily be included in a program, and nuclear stopping powers as calculated by Ziegler [2].

Using this code the energy spread, in percent of the mean scattered energy, was calculated for the case of C ions on Au films of different thickness, as shown in Fig. 5. As can be seen in the figure, with the 85 nm film used here, the energy spread is less than 10% only for a beam energy > 7 MeV. If a smaller spread is desired for lower energies, a thinner target must be used, for instance with a 25 nm thickness. For ions heavier than C, the stopping powers generally become larger, so the ions' energy spread in the Au will be greater.

In the present experiment carbon ions of eight bombarding energies were used: 1.5, 3.0, 4.5, 6.0, 7.5, 9.0, 10.5, and 12.0 MeV. The corresponding calculated mean energies E_{mean} at the detector were 1.03, 2.15, 3.30, 4.47, 5.64, 6.81, 7.99, and 9.17 MeV. Figure 6 concentrates the eight spectra from the surface barrier detector. The sixteen calculated $E_{\max}$ and $E_{\min}$ points served to calibrate the detector; they were fit with a straight line with a correlation coefficient of 0.9997. This is an indication of the overall consistency of the energy values used and the precision with which energies can be measured.

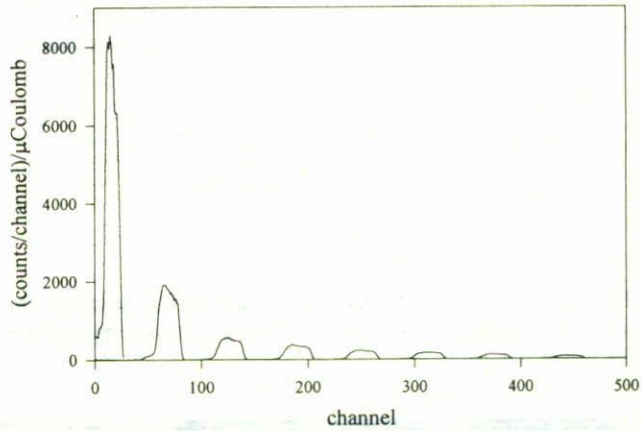

FIGURE 6. A superposition of the spectra measured in the surface barrier detector for the eight different energies.

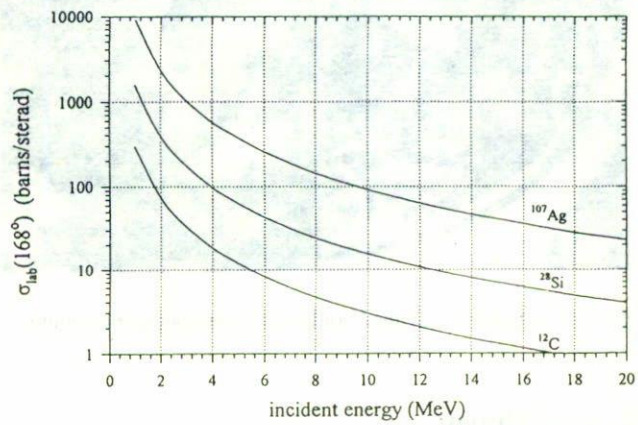

FIGURE 7. Calculated Coulomb laboratory cross sections for three different ions, representative of different mass intervals, at 168° laboratory angle.

Given a certain target, the Coulomb scattering cross section and the beam current will determine the duration of the experiment. Figure 7 shows the calculated laboratory cross sections for three different ions, representative of different mass intervals, at 168° laboratory angle. Since the cross sections are very large, in general an experiment will take only a few minutes. For the conditions of the present experiment, in order to obtain an easily readable track density of 100 mm^{-2} on the detector, the total beam charge collected on the target must be 4.8 μC, which for a typical current of 100 nA implies 48 s bombarding time. If ions of a charge state different from +1 are used, the calculated time is multiplied by the charge of the ions. In Fig. 6 the vertical axis was transformed to (counts/channel)/μC, so the Coulomb cross section is reproduced in the relative heights and shapes of the peaks.

In CR-39 the projected ranges R_0 of ions of the energies employed here are in the 1 to 20 μm interval. Figure 8 shows examples of projected ranges of ions in different mass regions, calculated using TRIM, assuming the density of CR-39 to be 1.32 g/cm^3. The latent track lengths are expected to

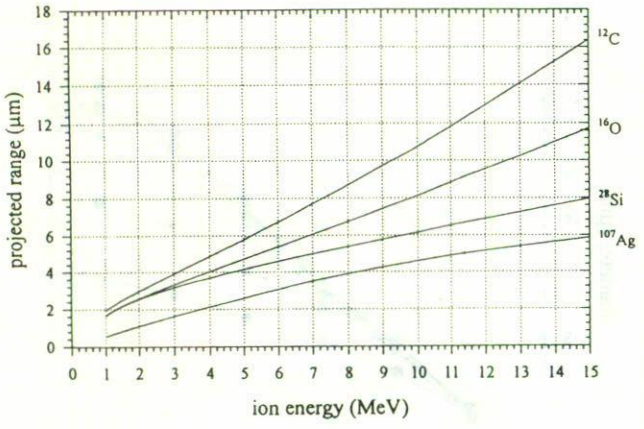

FIGURE 8. Examples of projected ranges of ions in different mass regions, calculated using TRIM.

to be essentially equal to the projected ranges. For the etching rates normally used, in the present case of 1,8 μm/hr in the bulk, the developed tracks can be studied when the cone depth is smaller than, equal to, or larger than the latent track length. This provides a useful procedure for studying the mechanisms of track etching. Furthermore, the distributions of ionization and structural damage along the ion path, produced by electronic and nuclear stopping respectively, can also be calculated using TRIM.

The detectors employed were 500 μm thick CR-39 with the 100 μm polyethylene protection removed, laser cut to 9.0 mm by 19.0 mm rectangles. At each energy three detectors were exposed, in order to try different etching procedures. The chemical etching was performed with 6.25 M KOH at 60° ± 2°C in varying time intervals, up to a total of 12 hours, and the circular track diameters (normal incidence) were measured at each interval using a digital image analysis system (DIAS) [10]. By measuring the change in thickness of the detector at different times, the bulk etching rate was estimated to be 1.8 μm/hr.

3. Results and discussion

The pit diameters measured for different etching times, as shown in Fig. 9, are plotted *vs.* mean ion energy in Fig. 10. The vertical error bars are those calculated by the image analysis system, and the horizontal bars correspond to the width of the energy peaks measured in the spectra.

The C ion ranges within the detector material can be observed in Fig. 8 to be in the 1 to 18 μm interval. Therefore, depending on the ion energy, for short etching times the bulk etching is less than the latent track length. After a certain time, the process switches to the regime in which the bulk etching is greater than the latent track length. Furthermore, the corresponding straggling values, as calculated by TRIM, are in the 100 to 300 nm interval, which means less than 5% of the range, except for the lowest energy. Therefore the ranges of the individual tracks are very close to one another.

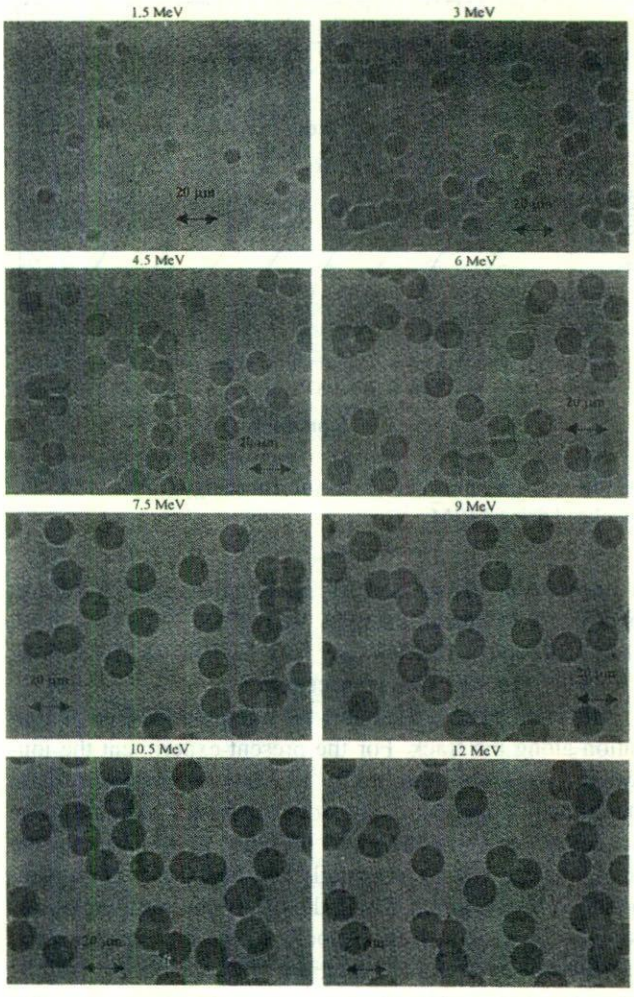

FIGURE 9. Etched tracks for different energies with 12 h etching time.

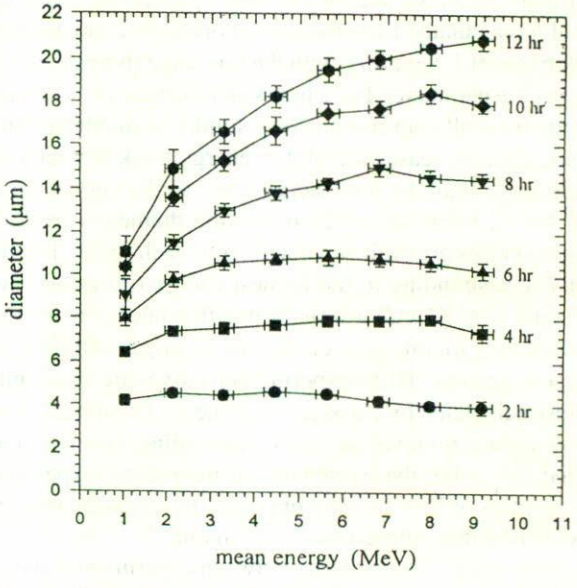

FIGURE 10. The pit diameters measured for different etching times, plotted *vs.* mean ion energy.

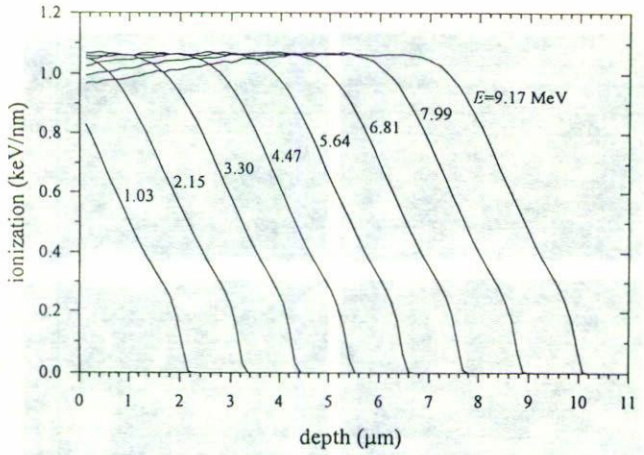

FIGURE 11. Ionization curves of different energy C ions in CR-39, calculated using TRIM.

In the present experiment the projected ranges R_0 corresponding to the mean energies 1.03, 2.15, 3.30, 4.47, 5.64, 6.81, 7.99, and 9.17 MeV are 1.97, 3.10, 4.18, 5.28, 6.38, 7.50, 8.66, and 9.87 μm, respectively.

The code TRIM calculates the energy deposited as ionization along the track. For the present experiment the ionization curves, depicted in Fig. 11, show an almost constant rate of energy deposit, rising slowly up to a maximum value at a certain residual energy of the ions, at which point the curve falls off with an essentially constant slope. This corresponds to the region in which the electronic stopping power increases linearly with the velocity of the ions, at low energies. It is not a product of straggling. These same curves show that the surface ionization turned out to be almost the same (close to 1 keV/nm) for all the energies considered. Nuclear stopping is approximately two orders of magnitude smaller than electronic stopping.

Figure 12 shows the pit diameters plotted *vs.* surface removal h (calculated from the corresponding etching time and an etch rate of 1.8 μm/hr), with the ion range (for each ion energy) as the parameter. For 2 hours etching time ($h = 3.6\,\mu$m) the pits from all energies are very similar in diameter, but as etching time increases the higher energy track diameters increase faster than the low energy ones, so the curves fan out until for 12 hours ($h = 21.6\,\mu$m) the diameters from different energies are well separated from each other. The data points corresponding to the highest energy (projected range 9.87 μm) were fit with a straight line that intersects the ordinate axis at 0.43 μm, close enough to the origin within the experimental errors. These experimental curves are very similar to those calculated by classical track theory [3] of track diameter *vs* surface removal, so the corresponding calculation was carried out, using the parameters of the present experiment, and the plots of Fig. 13 were obtained. For a reasonable fit to the experimental points a ratio of etch rates $V = V_{\text{Track}}/V_{\text{Bulk}}$ of 1.8 was used. The similarity between experimental and calculated curves indicates that the theory explains the etching process well.

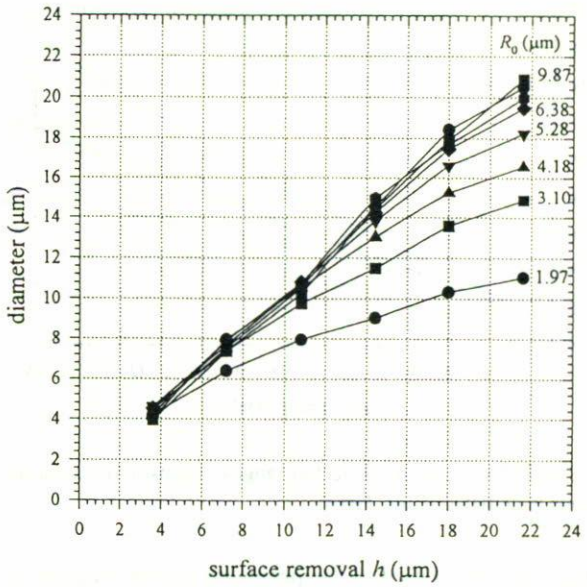

FIGURE 12. Measured track diameters plotted *vs.* surface removal h with the energy dependent ion range as the parameter.

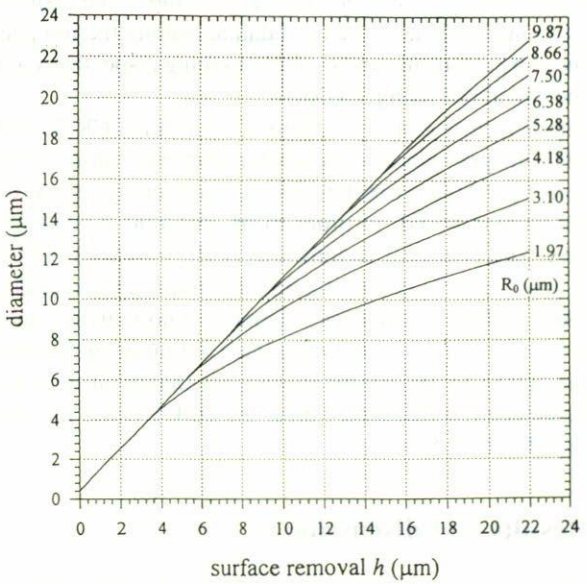

FIGURE 13. Calculation of track diameters using classical track theory. A reasonable fit to the experimental points was obtained with $V = 1.8$.

4. Conclusions

The usefulness of a low energy, multiple ion accelerator for the study of the mechanisms of track formation of ions in plastic detectors has been assessed. In combination with the backscattering technique, ion energy, energy spread, cross section, and projected range, are all within adequate intervals for many types of ions, constituting an alternative method for ion detection.

CR-39 detectors were exposed to carbon ions of energies between 1 and 10 MeV. The measured pit diameters were plotted *vs.* ion energy for various etching times, and *vs.* surface removal for various projected ranges (energies). These last plots are similar to those obtained from calculations based on classical track theory.

Acknowledgments

The support of CONACYT Projects F036-E9109 and G0010-E9109 is acknowledged, as well as the technical assistance of K. López and A. Sanchez.

1. S.A. Durrani and R.K. Bull, *Solid State Nuclear Track Detection Principles, Methods and Applications*, (Pergamon Books, Oxford, 1987).
2. J.F. Ziegler, J.P. Biersack, and U. Littmark, *The Stopping and Range of Ions in Solids*, (Pergamon Press, New York, 1985).
3. G. Somogyi and S.A. Szalay, *Nucl. Instrum. Methods* **109** (1973) 211.
4. G. Somogyi, *Nucl. Instrum. Methods* **173** (1980) 21.
5. W. Enge, *Radiat. Measurements* **25** (1995) 11.
6. M. Sadowski *et al.*, *Radiat. Measurements* **28** (1997) 201.
7. M. Sadowski *et al.*, *Radiat. Measurements* **28** (1997) 207.
8. W.K. Chu, J.W. Mayer, and M.A. Nicolet, *Backscattering Spectrometry*, (Academic Press, New York, 1978).
9. E.C. Montenegro, S.A. Cruz, and C. Vargas-Aburto, *Phys. Letters* **92A** (1982) 195.
10. G. Espinosa, R.B. Gammage, K.E. Meyer, and C.S. Dudney, *Radiat. Prot. Dosimetry* **66** (1996) 363.